~~State of the art for Titanium-Stainless Steel dissimilar FSW joints~~

On the effect of sheets mutual position and copper interlayer in FSW of dissimilar Ti6Al4V-SS316L lap joints: mechanical properties and metallurgical characterization

Harikrishna Rana[1,a*], Rosa Di Lorenzo [1,b], Gianluca Buffa[1,c], Livan Fratini[1,d]

[1]Department of Engineering, University of Palermo, Viale Delle Scienze, 90128 Palermo, Italy.

[a]harikrishnasinh.rana@unipa.it, [b] rosa.dilorenzo@unipa.it, [c]gianluca.buffa@unipa.it, [d]livan.fratini@unipa.it

ABSTRACT

Technological advancements catering to the specific requirements of different industries have led to a rise in the use of multi-material components. Combining titanium and stainless steel can reduce the weight of components used for many industrial applications, making it a popular choice. Nonetheless, conventional arc welding methods tend to produce flaws such as brittle intermetallic compounds, pores, cracks, and other issues due to the significant differences in these alloys' thermal, physical, and chemical properties~~the thermal, physical, and chemical properties of these alloys~~. Friction stir welding (FSW) is a renowned solid-state joining technology for creating dissimilar material joints producing visco-plastic material flow at the interface. The present investigation compares Ti6Al4V/ SS 316L lap joints metallurgical and mechanical properties as a function of ~~the~~

Formatted: Not Superscript/ Subscript

Formatted: Not Superscript/ Subscript

~~parameters such as~~ velocity ratio, ~~skin stringer~~sheets mutual position ~~swap~~, and presence of a Cu interlayer. ~~A comprehensive report detailing the~~ The process mechanics and the impact of different strategies on intermetallic (IMC), grain morphology, intermittent phases, joint resistance, and microhardness ~~is presented.~~discussed. It was found that …

Commented [GB1]: Add a line on major findings

Keywords: FSW, Lap joint, Dissimilar joint, ~~Skin, Stringer~~, Titanium, Stainless steel, intermetallic, Material~~,~~ flow.

1 Introduction

The evolving notion of multi-material components has stimulated numerous endeavors to make use of the "right material at the right spot". This conception has fueled the development of more than a few novel technologies ~~like~~as~~,~~ solid state joining and processing, additive manufacturing, ~~solid state joining and processing, selective laser melting~~, etc. not long ago. These technological innovations with a broad application base in space, chemical, shipping, automotive, and transportation industries promise a huge potential with tailored multi-material structures and components[1, 2]. It seems quite unimaginable to manufacture a multi-material component without dissimilar material joining. However, along with ~~a~~ large interest, there are a lot of unanswered questions about dissimilar material concepts in these industries, wherein weight saving is directly translated to economical saving. For instance, whether it is a dissimilar joint between an actuator shaft made up of Ti and stainless steel (SS) bevel

gear in an airplane or Ti exhaust pipes and SS mufflers in an automotive, dissimilar joining provides not only economical advantages but high-performance design solution too [3-5]. In fact, ~~S~~such multi-material components ~~turn~~make the structure lighter and more economical simultaneously.

On the flip side of the coin, such benefits do not come without challenges. The mismatch of ~~their~~ the two materials coefficients of thermal expansion, which are 8.6×10^{-6} /ºC and 17.2×10^{-6} /ºC for Ti_6Al_4V and SS 316L, respectively, ensues in a joint with huge residual stress[6]. Additionally, the disparity in properties like density, melting point, chemical affinity, etc. plays a negative role too, during joining, and~~.~~ The ~~F~~formation of brittle intermetallic compounds (IMCs) such as TiFe, $Ti_5Fe_{17}Cr_5$, and $TiFe_2$, ~~etc.~~ owing to extreme heat input in case of fusion welding, is inevitable[7, 8]. To date, TIG, MIG, braze welding, diffusion welding, and laser welding technologies have been widely reported to fabricate such dissimilar material joints[7, 9-11]. Chen et al. [7] have reported the laser joint between Ti_6Al_4V and SS 201 producing a maximum of 150 MPa joint resistance, failed at the IMC layers. Likewise, Cheng et al [10] have reported the joint between Ti grade 4 and SS 304 using various combinations of braze welding, MIG, and TIG welding, wherein all the samples fractured from the interface along the IMC layer when subjected to tensile loading. Upon loading the component, fractures have a tendency to follow the IMC layer as the energy required for crack propagation reduces with an increase in brittleness[8]. Hence, it is imperative to reduce the heat

Commented [GB2]: Numbers should not be subscript, please change it all through the paper

while joining these multi-material components and get rid of IMCs. One of the feasible solutions to suppress the reaction between SS and Ti is to use an interlayer that works as a diffusion barrier. Although numerous kinds of interlayers reported for SS/Ti joints with different techniques are V, Ta in laser welding[7], Ni, Cu, Al, and Ag in diffusion bonding[12-17], Ag-Cu, Cu-Ti, Ag-Cu-Zn, Ag, Ti-based alloy in brazing[18-20], none of these investigations reported bonding interface free from IMCs or defects. The study by Atasoy et al.[17] reported the absence of IMCs utilizing a silver-based interlayer, and the produced joints showed a maximum tensile strength of 32 MPa. On the other hand, when an aluminum-based interlayer was used, the resulting joints had a maximum tensile strength of 183 MPa, but Al-Fe IMC formed at the interface between the stainless steel and the interlayer[16]. ~~Meanwhile~~In turn, the copper-based interlayer formed Cu-Ti and Cu-Fe IMCs and prevented the formation of Ti-Fe IMC [15], which led to a maximum shear strength of 105 MPa. Based on the above observations~~In brief~~, solid-state welding may be more suitable than fusion related ones, since major problems associated with melting can be eradicated.

Commented [GB3]: Is this number right? It seems too low!

In the last two decades, FSW has evolved as an effective solid-state technique to produce defect-free joints between materials having large disparities in terms of properties and compositions [21-23]. Such immaculate joints are possible by lower heat input mechanics as compared to both conventional and innovative fusion-based processes [24-26]. Fazel et al.[27] has reported the commercially pure Ti/SS 304 lap

joint experimenting with several processing conditions and achieved 73% joint efficiency. Although the amount of IMC (TiFe) was minimized as compared to other solid-state techniques (diffusion bonding), it was not possible to omit it completely. Additionally, at elevated temperatures, the higher IMC layer thickness along with Ti oxide layer formation reportedly degraded the joint properties. Hence, it is quite desirable to have a suitable interlayer along with the lowest possible heat input parameters for a successful Ti/SS FSW joint.

From the aforesaid facts and reports, it can be stated that successful Ti/SS joints proposed with FSW can have an unmatched potential in industries for numerous applications. However, only an extremely limited number of researches have focused on this topic so far, accompanied by the limited availability of suitable literature reporting a defect-free joint. The objective of the present investigation is to produce a defect-free ~~skin stringer~~ Ti_6Al_4V /SS 316L FSW lap joint experimenting with distinct low heat input processing conditions ~~like~~ obtained with varying velocity ratio. Additionally, the effect of the mutual position of the sheets to be welded and the presence of a~~s,~~ Cu interlayer, ~~positions swap, etc.,~~was also investigated. The main mechanical and metallurgical properties of the joints were~~ and investigate~~ highlighted by ~~influences on~~ the analysis of joint strength, microhardness, ~~and microstructural features like~~ grain morphology, and IMCs~~, etc~~.

2 Materials & Methods

Dissimilar lap joints were created between 2 mm thick austenitic stainless steel AISI 316L and 2 mm thick titanium alloy Ti_6Al_4V. The chemical compositions of the as-received materials are mentioned in Table 1.

Table 1. Chemical compositions for the substrates

WT %	Ti	Al	V	Fe	C	Cr	Mo	Mn	Ni	Si	Other
Ti-6Al-4V	87.7÷91	5.5÷6.75	3.5÷4.5	<0.4	<0.08	-	-	-	-	-	<2.1
SS 316L	-	-	-	61.9÷72	<0.03	16÷18	2÷3	<2	10÷14	<1	<9.1

Both the skin and stringer plate ~~was~~were ~~maintained~~ saw cut to~~at~~ an identical size of 140 × 90 mm. When employing FSW on high-strength alloys such as titanium alloys, selecting the appropriate tool material is crucial. The author has illustrated the effectiveness of W25Re compared to conventional tungsten carbide alloys like K10 and K10-K30 in this regard.[28]. The tool design is represented schematically in Fig. 1. ~~As it is considered that the introduction of Cu interlayer between skin and stringer causes a substantial heat loss to surroundings, those experiments were conducted at the highest VR only~~. The experiment summary with respective welding conditions is summarized in Table 2, wherein W refers to the configuration with Ti on top, while Wr (reverse) refers to the configuration with SS on top. All the experiments were made with position control mode keeping a constant tool tilt angle of 2.5º. As it is considered that the introduction of Cu interlayer between skin and stringer causes a substantial heat loss to surroundings, those experiments were conducted at the highest VR only.

Commented [GB4]: Citation stye consistency

Table 2. Experimental Summary with respective welding conditions

ID	A	B	C	D	D
Sub ID	W	W	W	W	0.2
	Wr	Wr	Wr	Wr	0.2 R
Tool Rotation (TR) rev. min^{-1}	500	600	700	800	800
Tool ~~Advance~~ Feed (TF~~A~~) mm min^{-1}	41	37	35	33	33
Velocity Ratio (VR)	12	16	20	24	24

The microstructure specimens were ~~prepared~~ obtained as per the ~~standard~~ metallographic specimen preparation standard. Kroll's reagent (HF 2 ml + HNO_3 6 ml + H_2O 92 ml) was used for etching Ti_6Al_4V sections, while Carpenters reagent ($FeCl_3$ 8.5gm + $CuCl_2$ 2.4 gm, HCL 122 ml+ HNO_3 6ml + C_2H_6O 122 ml) was used for AISI 316L section. ~~Various microstructural features such as~~ Ggrain morphologies, material flow patterns, IMC particles, fractured particles, and other compositional elements were examined through the use of optical microscopy (OM) (OLYMPUS, Model-Inverted Metallurgical Microscope GX51), scanning electron microscopy (SEM), and energy dispersive spectroscopy (Zeiss, Model: Ultra-55 SEM).

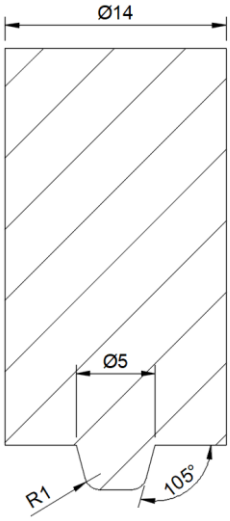

Fig. 1. W25Re tool geometry for FSW

To investigate microhardness, an Eseway 4302 Vickers hardness tester was used, following the ASTM E-384 standard. A square-based pyramid diamond indenter (136º intersects) was utilized with a 5 kg load and 15 seconds dwell time. For shear tests, specimens with a width of 10 mm were employed in a conventional tensile testing machine with a velocity of 2 mm min^{-1}.

3 Result & Discussion:

3.1 Macrostructural Characterization

The macrostructures of the prepared Ti/SS lap joints are displayed in Fig. 2. A considerable amount of skin thinning (ranging from 0.4 – 0.6 mm) was observed for the Ti skin specimens prepared with higher VR. Such thinning at higher VR can be attributed to increased material softening engendered by elevated temperatures at higher VR. This caused the substrate to lift at the front edge of the FSW tool ensuing the larger tool plunge in those specimens[29]. The SS 316L skin specimens were characterized with immaculate NZ, whereas the defect rate was increased with Ti_6Al_4V skin specimens and Cu interlayer specimens, respectively. Specimen prepared with VR ranging from 12 – 20 were characterized with minimal defect rate in the NZ, whereas the specimen prepared with VR of 24 were characterized with a larger proportion of defects such as porosities, voids, recesses, etc. Moreover, the specimen prepared with distinct processing conditions exhibited different material flow patterns ensuing in varied mechanical interlocking mechanisms. Specifically, extruded hooks varied in terms of dimensions, and profiles were identified in those specimens. Such hooks are formed due to discrete material flow patterns engendered owing to distinctive mechanical properties. The profile of the hook has a significant impact on the resulting properties because of the interlocking between the skin and stringer materials. It is

interesting to note that the phenomenon is prominent on the retreating side (RS) of the nugget. During FSW, the rotating tool pin pushes the stringer material underneath it, which extrudes in the opposite direction.

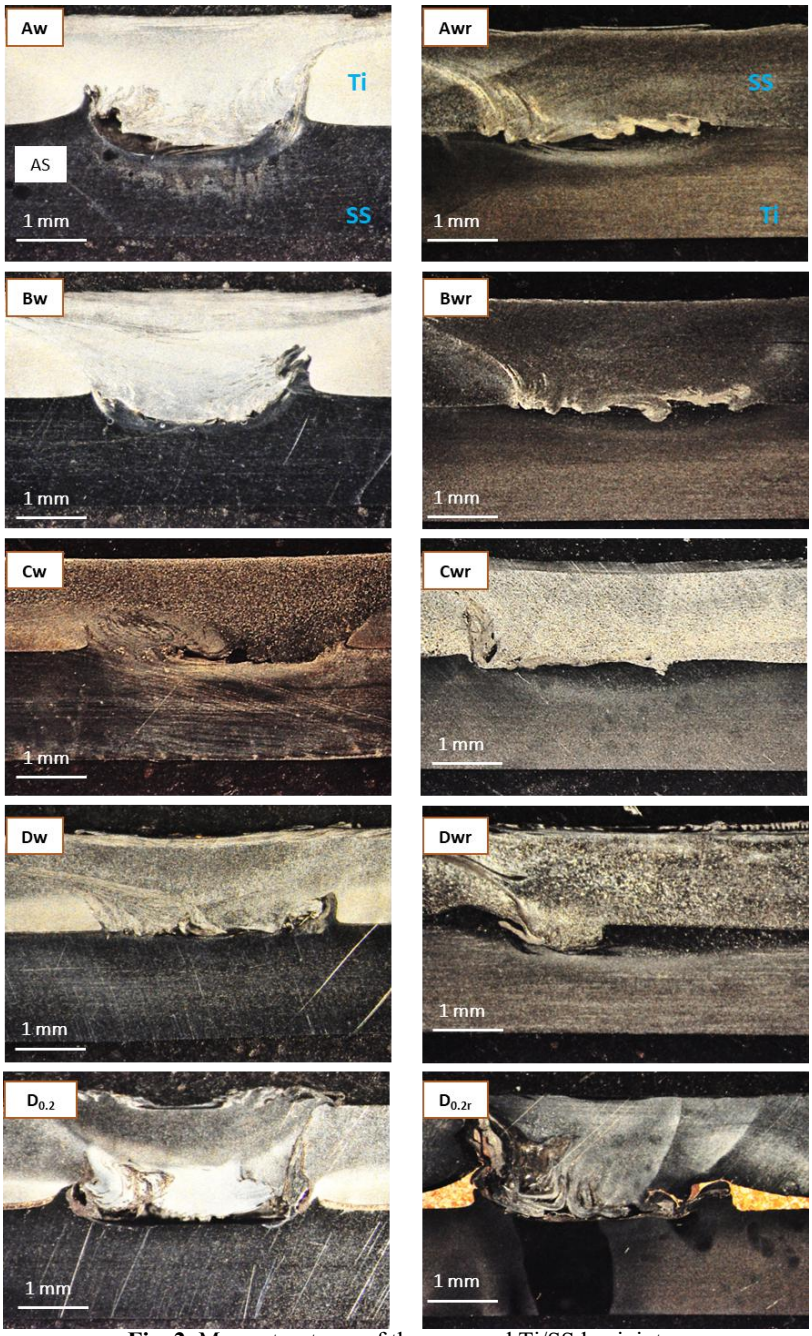

Fig. 2. Macrostructures of the prepared Ti/SS lap joints

Eventually, as the stringer material flows further upward being constrained and surrounded by the skin material, the extruded hook is engendered close to the thermo-mechanically affected zone (TMAZ). An identical phenomenon ensuing "extruded hook", has been reported during FSW of Al-Ti lap joint configurations[30].

Commented [GB5]: I think it could be useful to add a schematic image summing up this mechanics (before the one on the thermal flow)

On the one hand, the joints prepared without interlayer exhibited a limited SS material penetration to Ti skin or visa-versa accompanied by minimal defect generation. On the other hand, the joints prepared with the Cu interlayer exhibited larger SS material penetration to the Ti skin in the form of a hook. Simultaneously, the larger inflow of the SS material engenders a larger void into the stringer material and leaves behind a large cavity or a wormhole. Such a phenomenon can be justified by the heat transfer incurring for the two cases, one without interlayer and one with interlayer schematically. represented by Fig. 3 (a) and (b) respectively.

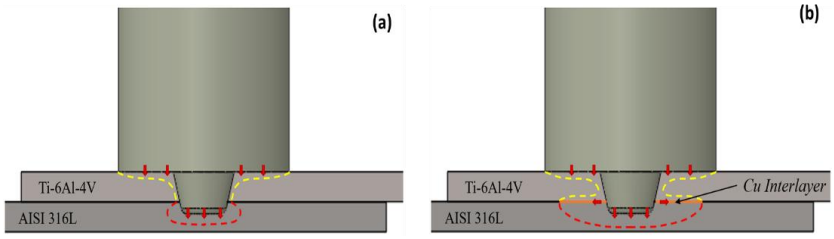

Fig. 3. Proposed heat flow during Ti/SS FSW for specimens prepared (a) Without Cu interlayer (b) With Cu interlayer.

The thermal conductivity of the titanium alloy is almost half that of stainless steel (k_Ti=6.70 W/(m K), k_SS=15 W/(m K)). This means that heat conducts more easily in SS substrate than Ti, resulting in a larger thermally influenced layer compared to Ti when no interlayer is present. Whereas, for the Ti skin the heat is concentrated at the center only with a very limited heat span. In the absence of an interlayer, the thermal layer in Ti remains near the interface, while in SS, there is a slight expansion of the thermal layer at the sides and under the pin. Introducing copper interlayer having substantially high thermal conductivity intensifies the rate of heat dissipation and conducts the fractional heat away from the NZ resulting in mechanical deformation instead of supposed material mixing at elevated temperatures. In the case of SS skin specimens joined with Cu interlayer, the Ti hook penetrated the softer SS skin to such an extent that it ended in the vicinity of the top skin surface and resulted in post-weld crack formation on the RS of the weld.

3.2 Microstructural Characterization

The micrographs for as-received commercially available Ti_6Al_4V titanium alloy and SS 316L substrates are displayed in Fig. 4(a). The SEM micrograph of Ti exhibited the bimodal microstructure consisting of αHCP + βBCC, wherein the majority of the area is occupied by the αHCP accompanied by uneven shapeless streak-like β patches [31]. The micrograph displays the α phase as dark because of its lower atomic number in comparison to the β phase, which appears brighter [31]. The micrograph of the SS

316L substrate was characterized by the majority of austenitic grains accompanied by a trivial number of ferritic ones. Annealing twins were found crossing grain boundaries at several locations. The grain size range for Ti was 2-10 µm, whereas for SS it was 25-30 µm.

3.2.1 Microstructure of Ti ~~skin SS Stringer Specimens~~on top joints

Highly diverse grain morphologies were observed in the different zones of the FSW joints prepared with different conditions as displayed in Fig. 4(b-d). Interestingly, for Ti skin specimens the NZ majorly occupied by the Ti was characterized by the larger grains as compared to the parent material (PM) in the central region, whereas the top and bottom-most regions were characterized with the finer grain structure (See Fig. 4(b)). Although the material at the shoulder-substrate interface experiences very high heat, it immediately gets air-cooled as it is exposed to the atmosphere upon the tool advance. Additionally, the Argon gas engaged for oxidation prevention further contributes to faster cooling, ensuing in the finest grain structure at the top region. The bottom-most region conducts the heat to the SS stringer through the interface ensuing in medium grains. However, the overall grain size in NZ was quite larger than in the PM. This can be attributed to the lower heat transfer coefficient of Ti which does not allow the heat to dissipate fast ensuing the larger grains led by the slow cooling rate.

Commented [GB6]: Skin and stringer, as far as I know, are used only for T joints. Please correct it through the paper

Commented [GB7]: Add this info to the materials and methods paragraph

Moreover, the microstructure of top regions ~~are~~ is composed of mixed structure viz., finer α + β lamellar, basket weave structure, and retained β phase. The center portion of the NZ was characterized by the alternate laths of α and β, whereas the bottom-most region was characterized by α' needles (See Fig. 4(b)). As indicated in earlier research, post-FSW air cooling leads to α + β lamellar and basket weave structure. The size of α and β lamella depends on the welding temperature and the residing time during which it remains above β transus temperature[32, 33]. These temperatures greatly rely on the welding conditions used during experiments. Moreover, the prevalent α + β lamellar microstructure throughout the NZ region indicates that the temperature surpassed β tarsus temperature in all those regions. The martensitic α'(HCP) needles which are a non-equilibrium condition of the α phase ensued owing to the occurrence of diffusion during transformation in the course of cooling from the temperature above β transus[34].

Commented [GB8]: Add ref

A clear grain morphological transition zone, namely the transition line zone (TLR) was identified between NZ and PM. This zone was characterized by a mixed and non-uniform microstructure composed of about 50% primary α-phase and 50% transformed β-phase (α+β lamellar). The appearance of the transformed β-phase in the HAZ indicates that the maximum temperature in this zone also exceeds the β-transus temperature. However, compared to the NZ, a lower volume fraction of the β phase indicates that the temperature was not high enough to fully cause the α to β

transformation during welding, which is attributed to a higher cooling rate in the thermally heated zone altered with respect to the agitation zone. The average grain size in the HAZ is approximately 18 µm.

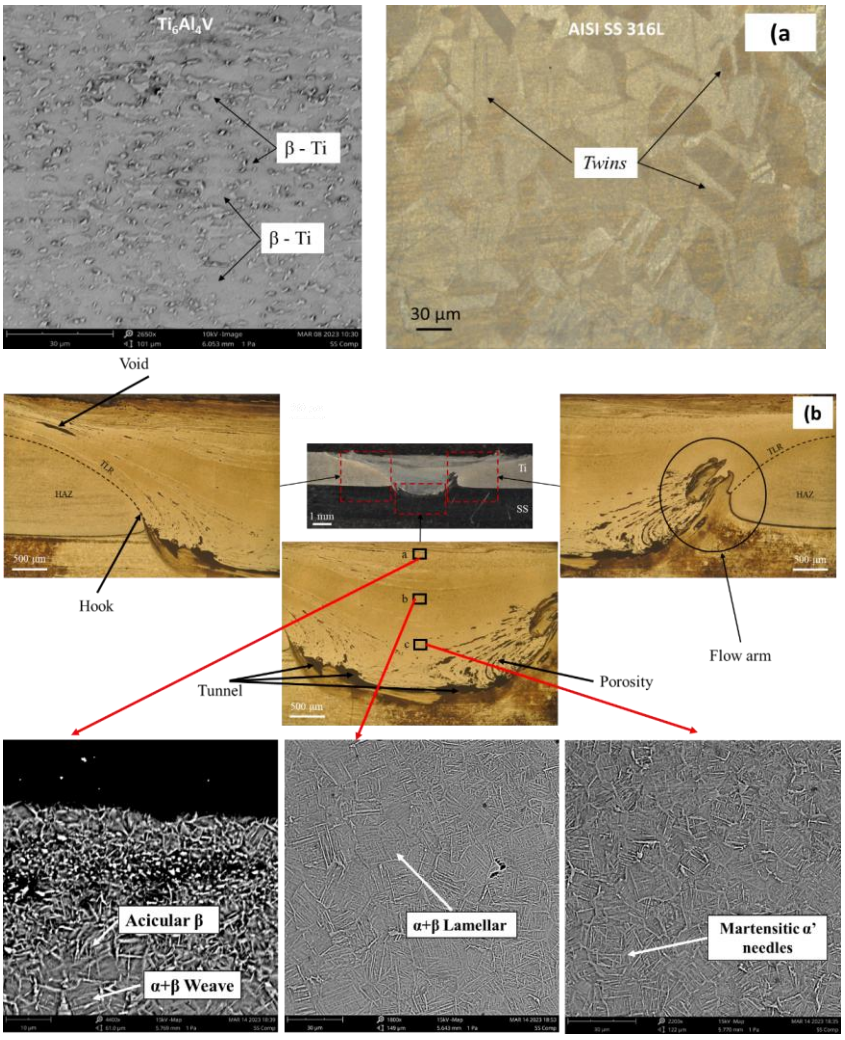

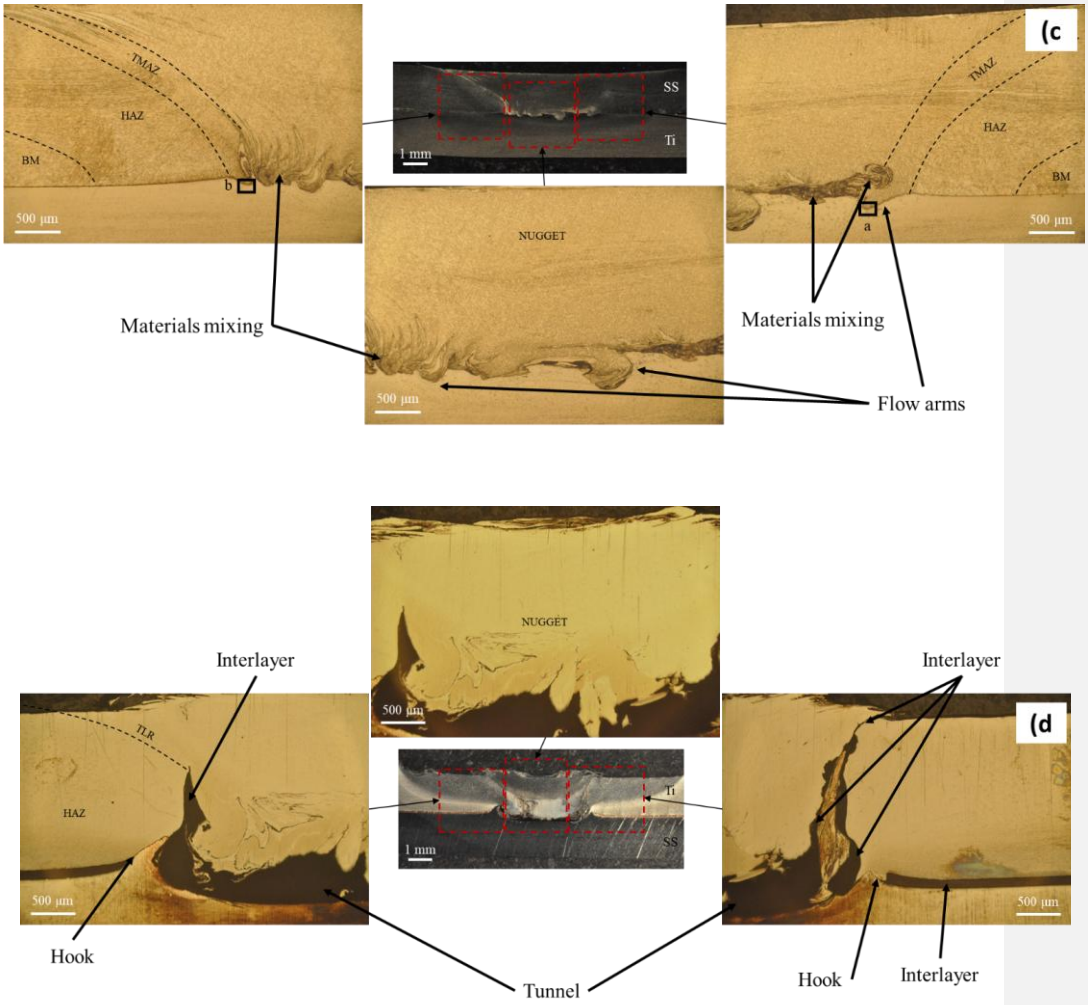

Fig. 4. Microstructural maps exhibiting distinct zones for (a) Parent Metal (b) Ti_6Al_4V skin specimen (B_w) (c) SS 316L skin specimen (B_{wr}) (d) Ti_6Al_4V skin specimen with Cu interlayer ($D_{0.2}$).

3.2.2 Microstructure of SS skin Ti Stringer Specimens

Formatted: Highlight

Various zones of the prepared SS skin specimens are displayed in Fig. 4(c). It is important to notice that the quantity of the twins has been largely reduced in the NZ of the specimen owing to the intense plastic deformation engendered by the rotating tool pin during the FSW process. Due to the imposed intense strain, the original twins undergo a crystallographic rotation and end up getting shattered [35]. Moreover, the topmost shoulder-substrate interaction region was characterized by ultra-fine grains owing to extreme shoulder-led deformation accompanied by rapid heating and cooling cycles experienced by the region[36]. However, the bottom region of NZ exhibited an onion ring structure wherein alternating layers of grains with varying sizes are noticed (See Fig. 4(c)). The FSW process resembles an extrusion process wherein each tool rotation leads to the extrusion of a plasticized layer in a semi-cylindrical shape. If the extruded layer is sliced, it may resemble the identical structure as observed in this region. Moreover, the elevated temperature along with the faster cooling cycle may engender the austenite-delta ferrite transition in several spots of NZ. Although the temperatures during FSW do not raise considerably high enough for such a transformation, the alloying elements present in the substrate may act as austenite stabilizers and bring down the transformation temperature. The delta ferrite has been reported as a precursor for the sigma phase formation during FSW of SS[37]. The sigma phase can formulate in the microstructure of SS in two scenarios. The first one involves

the direct transformation of the austenite phase into the sigma phase, which may not fit the current case as it requires prolonged thermal exposure. The second process involves the emergence of a ferrite /austenite duplex phase microstructure which can act as a catalyst for the sigma phase formation. Depending on the strain rate and thermal history the probability of a second scenario during FSW of SS is more prevalent. Apart, the SS skin specimens exhibited higher mechanical interlocking engendered by the SS flow arms penetrated in the Ti stringer. These specimens were majorly characterised free from the defects like porosity, cavity, or tunnel. Moreover, the number of flow arms were also higher as compared to the earlier case of Ti skin.

Formatted: Highlight

3.2.3 Microstructure of Ti skin Specimen with Cu interlayer

Fig. 5 exhibits the Ti/Cu/SS interface SEM micrograph along with the EDS elemental mapping results. From the elemental map exhibiting 49.2 wt.% Ti and 32.4 wt.% Cu confirms the probability of Ti_2Cu IMC formation at the interface. Fig. 5 clearly shows that the Cu interlayer efficiently prevented the formation of brittle Ti-Fe phases at the interface, and there are no intermetallic compounds present on the Ti side. It is reported for the Ti_6Al_4V/SS 316L diffusion joining that the planner nature of the Fe/Cu bonding interface limits the diffusion of Fe into Cu at the interface zone, preventing the formation of Fe-Cu-based IMCs thereby [14].

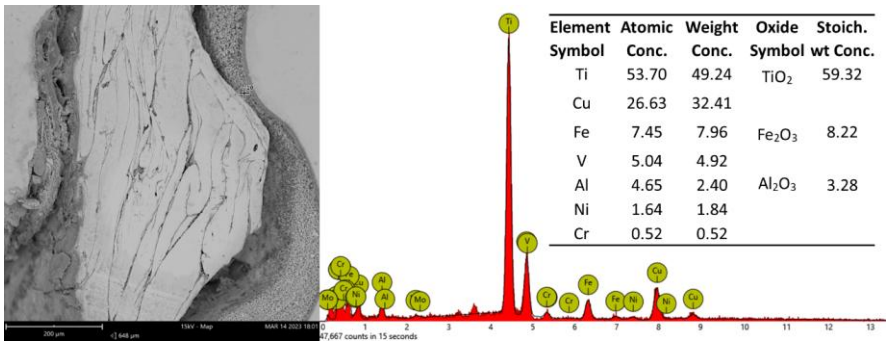

Fig. 5 Elemental Mapping at Ti/SS interface with Cu Interlayer

3.2.4 Interfacial Characterizations

In the course of FSW experiments, the peak temperature measured with help of an external thermocouple was in the range of 1075 – 1150 ºC which is sufficient for the elemental diffusion between SS 316L and Ti_6Al_4V. Such diffusion ultimately gave rise to the formation of a thin layer of TiFe-based IMC at the joint interface. According to the EDS map analysis results displayed in Fig. 6, it appears that a lean TiFe- based IMC was generated at the interface of Ti/SS. Identical IMC formation across the interface has been reported earlier with FSW and alternative solid-state joining methodologies[27, 38]. As the temperature rises, elemental migrations across the interface increase, facilitating the reaction between Ti and Fe and leading to the formation of a TiFe-based IMC phase. According to Ti-Fe binary phase diagram, at the temperature range mentioned mainly two IMCs may prevail, namely TiFe and $TiFe_2$[39]. Hence, it is

Commented [GB9]: Add also this to the mat & methods par, including position schematized in fig 1 (make a (b)

comprehensible that during FSW, the interfacial reaction between Ti and Fe results in the preferential formation of the TiFe phase at the interface. Upon the examination of joints produced at VR of 16, the thickness of the IMC layer was found to be 0.9 µm which is quite minimal as compared to alternative joining technologies (9 - 30 µm). Although it was discovered that the IMC layer thickness was increased with increasing the VR from 16 to 24, it did not surpass 3 µm. In contrast, when bonding dissimilar joints through diffusion, it is common to see a comparatively thicker layer being formed at the interface [17]. For instance, a TiFe-based IMC layer having a thickness of 6 µm was identified when CP-Ti was bonded to 304 SS using the lowest applied time and temperature [20]. As the high-temperature dwell time of the NZ in the FSW technique is relatively short, diffusion is restricted, which results in the expectation of a thinner interface layer.

Commented [GB10]: Also here ref needed (even the same of intro)

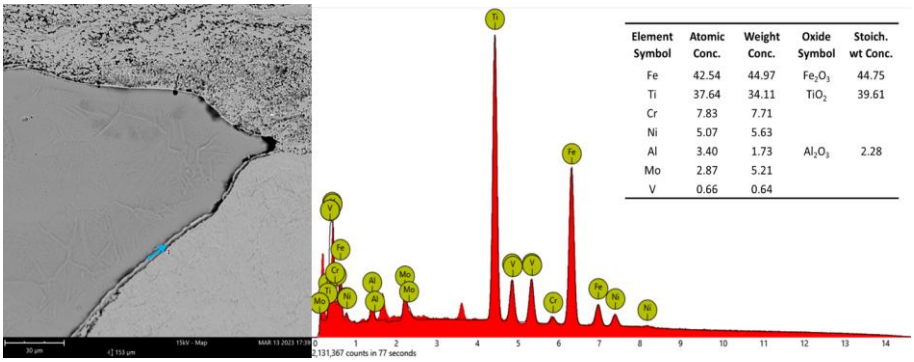

Fig. 6. Elemental Mapping at Ti/SS interface.

During the process, the rotating tool pin fragmented the interfacial portion of the Ti material and transferred it to the SS 316L side, resulting in the formation of a composite-like structure. This structure consists of an SS 316L matrix reinforced with the hard Ti particulates (detected through EDS) found near the interface. Those particulates were observed to align with the local material flow directions within the center of the NZ, near the interface (as shown in Fig. 7).

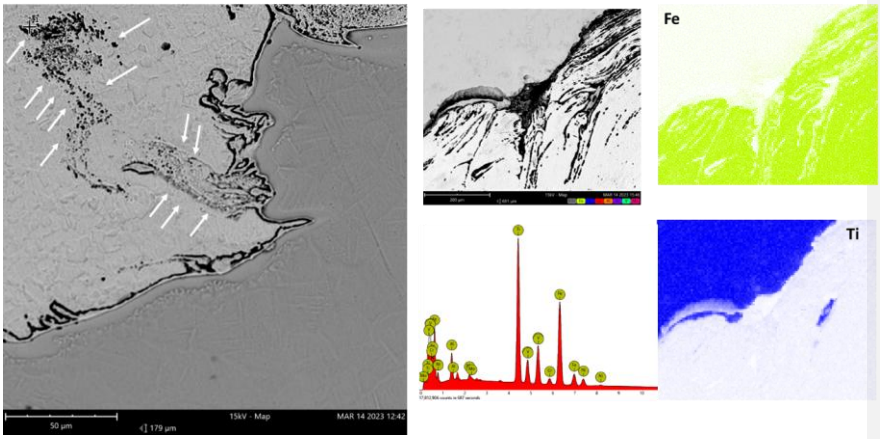

Fig. 7. Composite microstructure along the interface exhibiting Ti fragments in SS 316L matrix.

Apart, in Fig. 8 the micrograph displays EDS point-scan locations and the EDS element map across the SS-Ti interface at those spots for the FSW SS skin specimen (B_{wr}). A closer observation shows the diffusion depth of Fe into Ti is more than that of Ti into Fe. Such a phenomenon can be explained by the higher activation energy (293.2 KJ mol^{-1}) required for diffusion of Ti in Fe as compared to Fe in Ti (144.2 KJ mol^{-1}), ensuing higher diffusion coefficient of Fe in Ti as compared to Ti in Fe. The elements like Fe, Al, Ti, Cr, and Ni are observed at the SS-Ti interface as depicted in Fig. 8. These elements' presence is also noticed in β-Ti (in the vicinity of the SS-Ti interface) and rapidly declines further into the Ti side. Considering the peak temperature reported at the SS-Ti interface for VR of 22 during lap FSW of Ti-SS was 1075 - 1085 ºC, the current specimen Bwr which was prepared at VR of 16 is expected to engender a peak temperature of less than 1075 ºC. As per the Ti-Fe-Cr ternary diagram reported by Wang et al.[40], the β-transus temperature for Ti_6Al_4V is 980 ºC. Nonetheless, according to the Ti-Fe-Cr system at 800 ºC, only when the Fe or Cr wt% is greater than 5% α-Ti is transformed to β-Ti. This phenomenon indicates that the higher Fe and Cr content in Ti brings down the β- transus temperature. As the substrate materials heat up in FSW, it is believed that the Fe and Cr from SS are diffused to Ti_6Al_4V and enforce α-Ti to β-Ti transformation. The β-Ti is further transformed back to α-Ti in the region with lower Fe and Cr content while cooling ensuing α'-Ti needles near spots 7 and 8

(See Fig. 4(b)). Further, β-Ti is completely transformed to α-Ti at spots 9 – 12 owing to the absence of Fe and Cr elements.

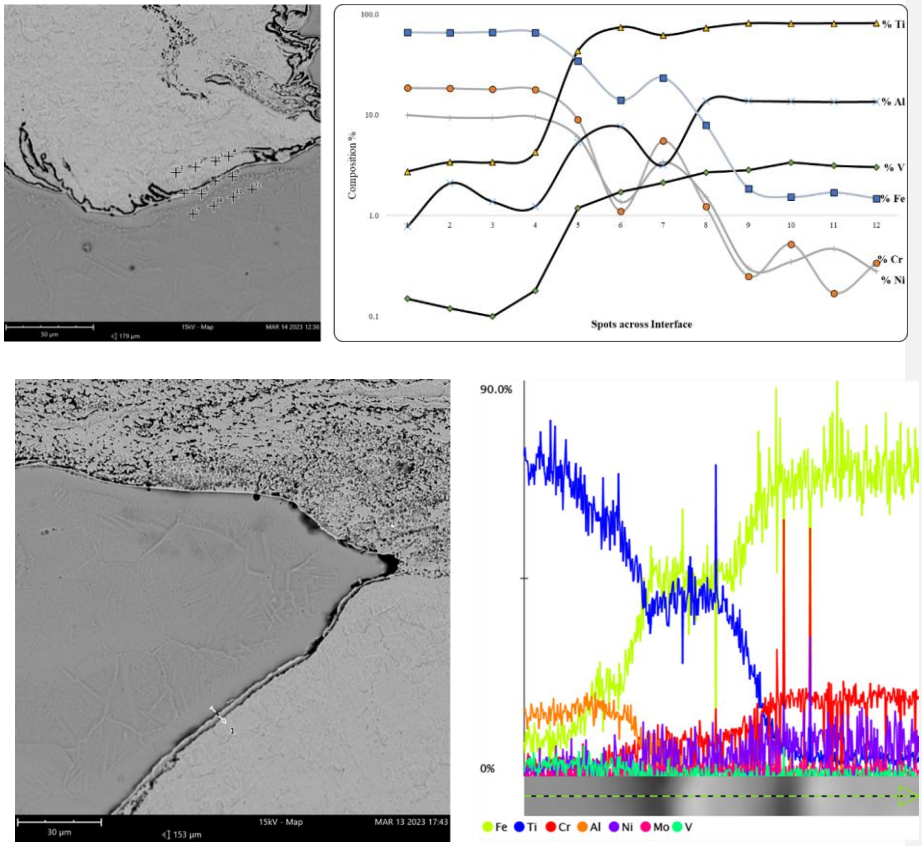

Fig. 8. SEM-EDS point scan along the Ti-SS interface and concentration profiles of the principal elements across the area.

Commented [GB11]: Figure needs larger fonts

3.3 Mechanical Properties

The tensile shear strength (TSS) results for all specimens are represented graphically in Fig. 9(a). Overall, the specimen prepared with SS skin exhibited the highest TSS followed by the Ti skin and Cu interlayer specimens. A typical "C" curve was followed for TSS concerning an increase in the VR from 12 – 24. Specimen B prepared at VR of 16 exhibited the highest TSS of 554 N/mm among all the specimens owing to almost defect-free microstructure, grain refinement, and the supreme mechanical interlocking offered by SS flow arms. The SS skin specimens exhibited considerable grain refinement, whereas the Ti skin specimens exhibited grain growth in the NZ of the prepared specimen. The lower strengths recorded in other specimens can be attributed to defects such as porosity, cavities, wormholes, and recesses. However, the dimensions and the quantity of the hooks in those specimens have greatly influenced the TSS results owing to the mechanical interlocking achieved. The specimens prepared with the 0.2 mm interlayer thickness offered a meager TSS which may have resulted from the two predominant mechanisms: (i) longer hook (ii) Reduction in the amount of FeTi brittle IMC, but a large recess at the interface.

As the hardness results are concerned, Ti_6Al_4V and SS 316L substrates displayed a hardness of ~275 HV and ~180 HV, respectively. The hardness mapping for the representative specimen (Condition B; VR - 16) is graphically represented in Fig. 9 (b). The NZ of SS and Ti skin specimens recorded a marginal rise of ~ 25% and 15% as

compared to the substrate, respectively. The improved hardness values can be attributed to the Ti-SS composite structure, and IMCs present in the NZ of the welded samples. However, several peaks in the hardness values were recorded in the vicinity of TMAZ for the specimen prepared with Ti skin, owing to the presence of hard and brittle IMCs. While the sudden fall in the hardness values can be attributed to the softer SS 316L hook formed near the TMAZ region. The observed increase in hardness values could be attributed to the effectiveness of shear lag and dislocation strengthening mechanisms. On the one side, the shear lag mechanism involves the transfer of load from the Ti matrix to the hard TiFe IMC present in the NZ. This generates shear stress at the interface, which restricts dislocation movement and improves material properties. On the other side, during the cooling period post-thermoplastic deformation caused by FSW, geometrically inexorable dislocations are formulated in the vicinity of the Ti/SS interface and IMCs due to the significant mismatch of coefficient of thermal expansion between two substrates. These dislocations impede crack propagation, which results in increased shear strength and hardness. In summary, the observed "dual" metallurgical-mechanical bonding mechanism accompanied by a comparatively lean IMC layer can be effective in producing dissimilar Ti/SS lap joints via FSW, making it a promising method for producing lap joints using dissimilar materials.

Commented [GB12]: This concept is more suited for the conclusions

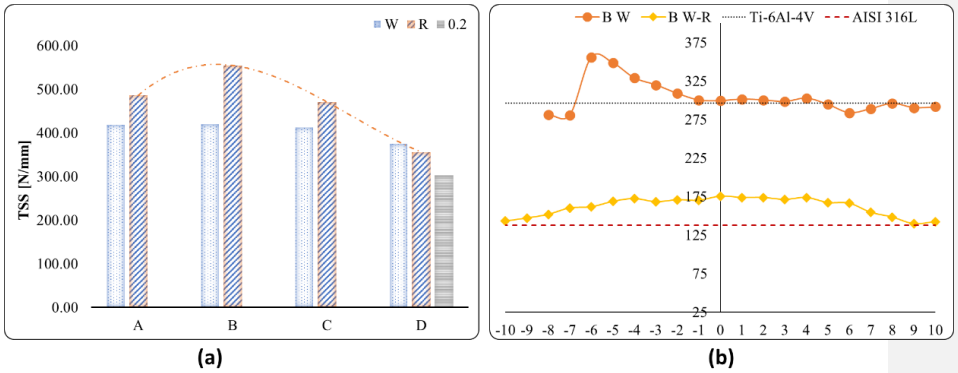

Fig. 9. Graphical comparison for (a) Tensile Shear strength (b) Hardness

Commented [GB13]: For which process conditions? This is not clear. From the text it seems that it is for the best performing (BWr), but in the legend you report both….not clear

4 Conclusions

The current ~~novel~~ investigation has reported successful dissimilar Ti_6Al_4V/ SS 316L lap joints using friction stir welding technology. The study has ~~extensively~~ examined the impact of several factors such as mutual sheet position, velocity ratio~~s~~, and the introduction of Cu interlayer on the joints' macrostructural, microstructural, and mechanical properties. The following conclusions have been drawn from the study:

- The lap joints created with SS 316L skin presented significantly superior outcomes as compared to ones with Titanium skin. The joints created with the latter configuration were identified with a few defects such as porosity and recess ensuing in comparatively lower outcomes.

- All the SS 316L skin specimens demonstrated almost flawless joints for all the processing velocity ratios. The peculiar material flow during the process has been outlined. Particularly the dimensions and quantity of extruded hook formed during the process significantly affected the tensile shear strength owing to the mechanical interlocking effect.
- Ti skin specimens exhibited overall larger grains as compared to the parent metal owing to a lower heat transfer coefficient, whereas SS 316L specimens exhibited finer grain structures in the joint areas. The nugget zone of the prepared joints was characterized by distinctive grains morphologies and phases in the different regions owing to different heating-cooling cycles experienced.
- The intermetallic layer thickness was influenced by the distinctive heat induced by various velocity ratios. The interface was majorly recognized with the FeTi intermetallic. Nevertheless, intermetallic layer thickness ranges from 0.9 – 1.2 µm indicating the superiority of the technology in terms of intermetallic suppression as compared to other solid-state and fusion-based joining technologies. Although sandwiching Cu interlayer between substrates aided in the suppression of brittle Fe-Ti-based intermetallic, those joints were characterized with a larger cavity and recess defects owing to the greater heat loss during FSW.
- A marginal rise of ~ 25% and 15% as compared to the substrate were recorded with SS and Ti skin specimens respectively. Such rise in the hardness was attributed

Commented [GB14]: In HV? With respect of?

to grain refinement, and intermetallic and composite structure present in the nugget zone of these joints. The SS 316L skin specimen prepared with a velocity ratio of 16 exhibited the highest tensile shear strength of 554 N/mm owing to the flawless nugget zone and superior interlocking offered by the multiple extruded hooks. These results are consistent/superior with the ones found in the literature for dissimilar lap joints prepared with both other solid-state and fusion based technologies.

5 References

[1] H. Gugel, A. Schuermann, W. Theisen, Laser welding of NiTi wires, Materials Science and Engineering: A, 481 (2008) 668-671.
[2] G. Kale, R. Patil, P. Gawade, Interdiffusion studies in titanium–304 stainless steel system, Journal of nuclear materials, 257 (1998) 44-50.
[3] S.M. Gilbert, Solid-state joining of titanium alloy to stainless steel, Colorado School of Mines, 2018.
[4] F.C. Campbell, Elements of metallurgy and engineering alloys, ASM International, 2008.
[5] A.C. Inc., MetalMiner Insights, in, Alpha Commodities Inc., Gary, IN 46403, 2022.
[6] C.Y. Ho, R.E. Taylor, Thermal expansion of solids, ASM international, 1998.
[7] S. Chen, M. Zhang, J. Huang, C. Cui, H. Zhang, X. Zhao, Microstructures and mechanical property of laser butt welding of titanium alloy to stainless steel, Mater. Des, 53 (2014) 504-511.
[8] B. Shanmugarajan, G. Padmanabham, Fusion welding studies using laser on Ti–SS dissimilar combination, Optics and Lasers in Engineering, 50 (2012) 1621-1627.
[9] X. Yue, P. He, J. Feng, J. Zhang, F. Zhu, Microstructure and interfacial reactions of vacuum brazing titanium alloy to stainless steel using an AgCuTi filler metal, Mater. Charact., 59 (2008) 1721-1727.
[10] Z. Cheng, J. Huang, Z. Ye, H. Liu, J. Yang, S. Chen, X. Zhao, Interfacial microstructure evolution and mechanical properties of TC4 alloy/304 stainless steel joints with different joining modes, Journal of Manufacturing Processes, 36 (2018) 115-125.
[11] R. Shiue, S. Wu, J. Shiue, Infrared brazing of Ti–6Al–4V and 17-4 PH stainless steel with (Ni)/Cr barrier layer (s), Materials Science and Engineering: A, 488 (2008) 186-194.

[12] S. Kundu, B. Mishra, D. Olson, S. Chatterjee, Interfacial reactions and strength properties of diffusion bonded joints of Ti64 alloy and 17-4PH stainless steel using nickel alloy interlayer, Mater. Des, 51 (2013) 714-722.
[13] S. Kundu, S. Chatterjee, Characterization of diffusion bonded joint between titanium and 304 stainless steel using a Ni interlayer, Mater. Charact., 59 (2008) 631-637.
[14] S. Kundu, M. Ghosh, A. Laik, K. Bhanumurthy, G. Kale, S. Chatterjee, Diffusion bonding of commercially pure titanium to 304 stainless steel using copper interlayer, Materials Science and Engineering: A, 407 (2005) 154-160.
[15] A. Elrefaey, W. Tillmann, Solid state diffusion bonding of titanium to steel using a copper base alloy as interlayer, J. Mater. Process. Technol., 209 (2009) 2746-2752.
[16] P. He, X. Yue, J. Zhang, Hot pressing diffusion bonding of a titanium alloy to a stainless steel with an aluminum alloy interlayer, Materials Science and Engineering: A, 486 (2008) 171-176.
[17] E. Atasoy, N. Kahraman, Diffusion bonding of commercially pure titanium to low carbon steel using a silver interlayer, Mater. Charact., 59 (2008) 1481-1490.
[18] C. Liu, C. Ou, R. Shiue, The microstructural observation and wettability study of brazing Ti-6Al-4V and 304 stainless steel using three braze alloys, Journal of materials science, 37 (2002) 2225-2235.
[19] H. Dong, Z. Yang, Z. Wang, D. Deng, C. Dong, CuTiNiZrV amorphous alloy foils for vacuum brazing of TiAl alloy to 40Cr steel, J. mater. sci. technol., 31 (2015) 217-222.
[20] T. Chung, K. Jungsoo, B. Jeongseok, R. Byoungho, N. Daegeun, Microstructures of brazing zone between titanium alloy and stainless steel using various filler metals, Transactions of Nonferrous Metals Society of China, 22 (2012) s639-s644.
[21] P. Patel, H. Rana, V. Badheka, V. Patel, W. Li, Effect of active heating and cooling on microstructure and mechanical properties of friction stir–welded dissimilar aluminium alloy and titanium butt joints, Weld. World., 64 (2020) 365-378.
[22] Y. Su, W. Li, F. Gao, A. Vairis, Effect of FSW process on anisotropic of titanium alloy T-joint, Mater. Manuf. Process, 37 (2022) 25-33.
[23] G. Buffa, M. De Lisi, E. Sciortino, L. Fratini, Dissimilar titanium/aluminum friction stir welding lap joints by experiments and numerical simulation, Adv. Manuf., 4 (2016) 287-295.
[24] M.P. Mubiayi, E.T. Akinlabi, Friction stir welding of dissimilar materials: an overview, in: Proceedings of World Academy of Science, Engineering and Technology, World Academy of Science, Engineering and Technology (WASET), 2013, pp. 65-69.
[25] P. Goel, N.Z. Khan, Z.A. Khan, A. Ahmari, N. Gangil, M.H. Abidi, A.N. Siddiquee, Investigation on material mixing during FSW of AA7475 to AISI304, Mater. Manuf. Process, 34 (2019) 192-200.

[26] J. Verma, R.V. Taiwade, C. Reddy, R.K. Khatirkar, Effect of friction stir welding process parameters on Mg-AZ31B/Al-AA6061 joints, Mater. Manuf. Process, 33 (2018) 308-314.
[27] M. Fazel-Najafabadi, S. Kashani-Bozorg, A. Zarei-Hanzaki, Joining of CP-Ti to 304 stainless steel using friction stir welding technique, Mater. Des, 31 (2010) 4800-4807.
[28] G. Buffa, L. Fratini, F. Micari, L. Settineri, On the choice of tool material in friction stir welding of titanium alloys, Proceedings of NAMRI/SME, 40 (2012).
[29] M. Yadava, R. Mishra, Y. Chen, B. Carlson, G. Grant, Study of friction stir joining of thin aluminium sheets in lap joint configuration, Sci. Technol. Weld. Join., 15 (2010) 70-75.
[30] Y. Chen, C. Liu, G. Liu, Study on the joining of titanium and aluminum dissimilar alloys by friction stir welding, Open Mater. Sci., 5 (2011) 6-10.
[31] A.K. Singh, B. Kumar, K. Jha, A. Astarita, A. Squillace, S. Franchitti, A. Arora, Friction stir welding of additively manufactured Ti-6Al-4V: microstructure and mechanical properties, J. Mater. Process. Technol., 277 (2020) 116433.
[32] Damisih, I.N. Jujur, J. Sah, Agustanhakri, D.H. Prajitno, Characteristics microstructure and microhardness of cast Ti-6Al-4V ELI for biomedical application submitted to solution treatment, in: AIP conference proceedings, AIP Publishing LLC, 2018, pp. 020037.
[33] B. Davis, F. Liou, Y. Huang, Study of grain size variation and saw-tooth spacing during machining of additively manufactured titanium alloy, MRS Communications, 5 (2015) 341-346.
[34] M. Esmaily, S.N. Mortazavi, P. Todehfalah, M. Rashidi, Microstructural characterization and formation of α′ martensite phase in Ti–6Al–4V alloy butt joints produced by friction stir and gas tungsten arc welding processes, Mater. Des, 47 (2013) 143-150.
[35] M. Hajian, A. Abdollah-Zadeh, S. Rezaei-Nejad, H. Assadi, S. Hadavi, K. Chung, M. Shokouhimehr, Microstructure and mechanical properties of friction stir processed AISI 316L stainless steel, Mater. Des, 67 (2015) 82-94.
[36] M. Costa, D. Verdera, M. Vieira, D. Rodrigues, Surface enhancement of cold work tool steels by friction stir processing with a pinless tool, Applied surface science, 296 (2014) 214-220.
[37] S.H.C. Park, Y.S. Sato, H. Kokawa, K. Okamoto, S. Hirano, M. Inagaki, Rapid formation of the sigma phase in 304 stainless steel during friction stir welding, Scr. Mater, 49 (2003) 1175-1180.
[38] S. Kundu, S. Chatterjee, Diffusion bonding between commercially pure titanium and micro-duplex stainless steel, Materials Science and Engineering: A, 480 (2008) 316-322.

[39] M. Ghosh, K. Bhanumurthy, G. Kale, J. Krishnan, S. Chatterjee, Diffusion bonding of titanium to 304 stainless steel, Journal of nuclear materials, 322 (2003) 235-241.
[40] S. Wang, K. Wang, G. Chen, Z. Li, Z. Qin, X. Lu, C. Li, Thermodynamic modeling of Ti-Fe-Cr ternary system, Calphad, 56 (2017) 160-168.